Relative Solution Electron Affinities of Selectively Deuteriated Pyrenes: Correlations between Voltammetric, Electron Paramagnetic Resonance, and Semiempirical PM3 Data

Ole Hammerich* and Merete F. Nielsen

Department of Chemistry, University of Copenhagen, Symbion Science Park, Fruebjergvej 3, DK-2100 Copenhagen, Denmark

Han Zuilhof, Patrick P. J. Mulder, and Gerrit Lodder*

Leiden Institute of Chemistry, Gorlaeus Laboratories, Leiden University, P.O. Box 9502, 2300 RA Leiden, The Netherlands

Richard C. Reiter,* David E. Kage, Charles V. Rice, and Cheryl D. Stevenson*

Department of Chemistry, Illinois State University, Normal, Illinois 61790-4160

Received: July 25, 1995; In Final Form: October 5, 1995[⊗]

The equilibrium isotope effects (EIE) for the one-electron transfer between pyrene and seven regioselectively deuteriated pyrene isotopic isomers in dimethylformamide with 0.1 M tetrabutylammonium hexafluorophosphate were measured electrochemically. These data correlate linearly with the free energies ($\Delta G°$) obtained in tetrahydrofuran using electron paramagnetic resonance (EPR) techniques. However, the slope of the resulting line is not unity, and it indicates that the EIE in the DMF system is only two-thirds of that in the THF system. PM3 calculated $\Delta G°$'s, which would correspond to the gas phase electron transfers, also correlate linearly with both sets of experimental data, but the predicted magnitudes of the EIE's are smaller than those observed experimentally by either technique. The nonunity slopes probably reflect slight differences in ion solvation and/or ion association parameters between the anion radicals of the isotopic isomers. No general relationship between the EIE and the charge on the hydrogen/deuterium substituted carbon atom was found.

Introduction

The effect of deuterium substitution on the reduction potential of aromatic compounds has recently been studied in great detail, both experimentally and theoretically. Electron paramagnetic resonance (EPR), electrochemical, and other studies have shown that the electron-accepting ability of polycyclic aromatic hydrocarbons decreases upon deuteriation.[1] That is, the standard free energy change of reaction 1, where A and *A represent the isotopically light and heavy analogues, respectively, is positive.

$$A^{\bullet -} + {}^*A \rightleftarrows A + {}^*A^{\bullet -} \qquad (1)$$

The existence of this deuterium isotope effect on the electron affinity has been confirmed by a variety of techniques, among them NMR,[2] ion cyclotron resonance,[3] mass spectrometry,[4] and cyclic voltammetry.[1b,5] The endothermicity has been explained in terms of the extra electron being added to an antibonding π^*-orbital, which reduces the total bonding.[1a,4] In agreement with the general rule that "the lighter isotope prefers the looser species", the equilibrium of reaction 1 lies to the left. The magnitude of the effect is dependent on the number of isotopically substituted sites.[6] For example, the more deuteriums on the benzene ring, the more positive is the reaction enthalpy for electron transfer from the benzene anion radical to deuteriated benzene.[6]

The magnitude of the effect has also been linked to the spin and charge density at the isotopically substituted carbon atom. From the study of a series of perdeuteriated polycyclic aromatic hydrocarbons, Stevenson and Sturgeon concluded that deuterium substitution on carbon atoms with larger charge densities in the radical anion yields smaller K_{eq} values.[7] This conclusion was reinforced by the observation of a linear free energy relationship for reaction 2.[8]

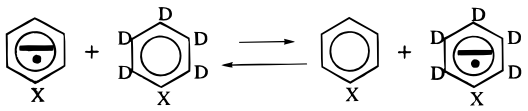

(2)

When X represents an electron-donating substituent, K_{eq} for reaction 2 is smaller than it is when X represents an electron-withdrawing substituent. The substituent causes variations in the total excess charge density from the antibonding electron in the part of the molecule where isotopic substitution has taken place. With electron-withdrawing substituents this excess is smaller, and the influence of isotopic substitution is therefore smaller.

Two reports have been published that give some theoretical clarification of the effect.[9,10] Marx, Kleinhesselink, and Wolfsberg performed calculations using empirical values of force constants and concluded that the deuterium isotope effects, where X = NO_2 and H, are explicable in terms of standard isotope theory.[9] Zuilhof and Lodder later reported analogous calculations of the isotope effects on the reaction enthalpy in which the force constants were quantum mechanically derived.[10] The latter authors concluded that the overall isotope effect was the sum of many small, and often oppositely directed, vibrational changes. For the case where A represents benzene or pyrene (**1a**) and *A represents perdeuteriated benzene or perdeuteriated pyrene (**1h**) in reaction 1, they found no obvious relationship between the amount of charge residing on a carbon atom and the magnitude of $\Delta G°$. This $\Delta G°$ was assumed to be identical to $\Delta H°$ as $\Delta S° = 0$.

[⊗] Abstract published in *Advance ACS Abstracts,* February 1, 1996.

0022-3654/96/20100-3454$12.00/0

In view of the widespread interest regarding this equilibrium isotope effect,[1b−e,5,9,10] we were motivated to further investigate the correlation of experimental K_{eq}'s for reaction 1 with theoretically computed K_{eq}'s and with charge distributions in the anion radicals. Seven specifically deuteriated pyrene isotopic isomers (structures **1b**−**1g** and perdeuteriated pyrene (**1h**), as a precursor to **1f**) were synthesized, and the $\Delta G°$ values for reaction 1, where A = pyrene and *A = **1b**−**1h**, were measured electrochemically and by EPR, a technique that has frequently been used to determine $\Delta G°$ values for electron transfer reactions.[11] This was complimented by the calculation

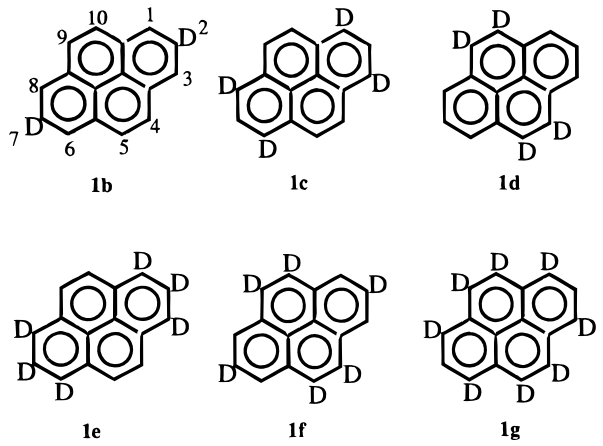

of the reaction enthalpies using semiempirical PM3 MO calculations.[12]

Results

EPR Experiments. The EPR technique for the determination of relative solution electron affinities,[11a−e] which can also be utilized for H and D isotopic isomers,[13] was used to study the competitive electron transfer equilibria between pyrene and the partially deuteriated pyrenes. This technique obviously relies upon the detailed analysis of the EPR spectral patterns of the individual anion radicals involved, including those of any significant isotopic isomeric impurities.

*2,4,5,7,9,10-d_6-Pyrene (**1f**).* The potassium reduction of our synthesized 2,4,5,7,9,10-d_6-pyrene (pyrene = PY) in THF yields an anion radical solution that exhibits the expected EPR pattern from the desired 2,4,5,7,9,10-d_6-PY$^{\bullet-}$, but this anion radical only accounts for 74.6% of the spectral intensity. It is necessary to include an 18.6% 1,2,4,5,7,9,10-d_7-PY$^{\bullet-}$ and a 6.8% 2,4,5,7,9-d_5-PY$^{\bullet-}$ contribution (in accordance with Table 1) to obtain a simulation that is a good representation of the real EPR spectrum (see Figure 1; the a_H's and a_D's are given in Table 2).

Although the EPR spectrum of our potassium reduced sample of 2,4,5,7,9,10-d_6-PY is quite complex, it is very well simulated as can be seen in Figure 1. The hyperfine lines due to 2,4,5,7,9,10-d_6-PY$^{\bullet-}$ appear at magnetic fields where the hyperfine lines due to PY$^{\bullet-}$ are relatively intense. Thus, the mixtures of PY and 2,4,5,7,9,10-d_6-PY were biased heavily toward the deuteriated system in terms of relative concentrations. This allows good resolution of the 2,4,5,7,9,10-d_6-PY$^{\bullet-}$ spectrum while unperturbed hyperfine components from PY$^{\bullet-}$ can be found outside of the spectral region of 2,4,5,7,9,10-d_6-PY$^{\bullet-}$ (Figure 2).

A mixture of 79.3 mg of our (isotopically impure) 2,4,5,7,9,10-d_6-PY sample (79.3 × 0.746/208 = 0.284 mmol of **1f**) and 1.1 mg (0.005 45 mmol) of PY in 20 mL of THF was reduced with a very deficient amount of potassium metal and further diluted with THF. Upon EPR analysis (173 K), the resulting anion radical solution exhibited both expected anion radicals along with the impurity anion radicals mentioned above. The EPR spectrum (Figure 2) is best simulated with the ratio of the PY and 2,4,5,7,9,10-d_6-PY anion radicals being [2,4,5,7,9,10-d_6-

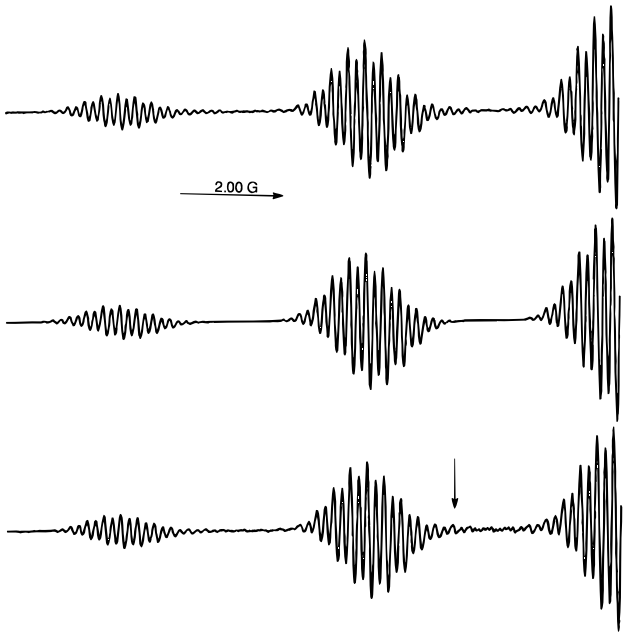

Figure 1. Upper: low-field half (a 12 G scan is shown) of the EPR spectrum of our sample of 2,4,5,7,9,10-d_6-pyrene at 173 K reduced with K in THF. Middle: computer simulation of the EPR spectrum for 2,4,5,7,9,10-d_6-PY$^{\bullet-}$ (coupling constants shown in Table 2). The presence of the isotopic impurities is not accounted for. Lower: computer simulation as above but including 76% 2,4,5,7,9,10-d_6-PY$^{\bullet-}$ in the presence of 18.6% 1,2,4,5,7,9,10-d_7-PY$^{\bullet-}$and 6.8% 2,4,5,7,9-d_5-PY$^{\bullet-}$ (Table 1). Note the improved agreement with the real spectrum (see, for example, the area indicated by the vertical arrow). The peak-to-peak line width (PPW) is 0.07 G.

TABLE 1: Molar Percentages (Normalized to 100%) of Various Deuteriated Species in Samples 1b−1g Used in Optimized EPR Simulations

desired compound	deuteriated species	% deuteriated species	
2,7-d_2-PY	2,7-d_2-PY	72.4	**1b**
	1,2,7-d_3-PY	4.1	
	2,4,7-d_3-PY	2.7	
	2-d_1-PY	4.7	
	2,4,5,7,9-d_5-PY	5.5	
	2,4,5,7,9,10-d_6-PY	3.1	
	misc d_4-PY's	7.5	
1,3,6,8-d_4-PY	1,3,6,8-d_4-PY	83.0	**1c**
	1,3,6-d_3-PY	17.0	
4,5,9,10-d_4-PY	4,5,9,10-d_4-PY	74.7	**1d**
	2,4,5,9,10-d_5-PY	14.3	
	4,5,9-d_3-PY	9.4	
	1,4,5,9,10-d_5-PY	1.6	
1,2,3,6,7,8,-d_6-PY	1,2,3,6,7,8-d_6-PY	58.8	**1e**
	1,2,3,4,6,7,8-d_7-PY	3.0	
	1,2,3,6,7-d_5-PY	8.6	
	1,2,3,4,6,7-d_6-PY	5.8	
	1,2,3,6,8-d_5-PY	4.3	
	1,2,3,4,6,8-d_6-PY	2.9	
	1,2,3,4,5,6,7,8-d_8-PY	6.9	
	1,2,3,4,5,6,7,8,9-d_9-PY	4.4	
	d_{10}-PY	2.3	
	misc d_4-PY's	2.9	
2,4,5,7,9,10-d_6-PY	2,4,5,7,9,10-d_6-PY	74.6	**1f**
	1,2,4,5,7,9,10-d_7-PY	18.6	
	2,4,5,7,9-d_5-PY	6.8	
1,3,4,5,6,8,9,10-d_8-PY	1,3,4,5,6,8,9,10-d_8-PY	61.7	**1g**
	1,2,3,4,5,6,8,9,10-d_8-PY	17.4	
	1,3,4,5,6,8,9-d_7-PY	15.5	
	1,3,4,5,6,9,10-d_7-PY	5.4	

TABLE 2: Coupling Constants in Gauss Used To Generate Simulations of the EPR Spectra

compound(s)	$a_{H1,3,6,8}$	$a_{H4,5,9,10}$	$a_{H2,7}$[a]	$a_{D1,3,6,8}$	$a_{D4,5,9,10}$	$a_{D2,7}$
1a, **1b**, **1d**−**f**, **1h**	4.818	2.130	1.012	0.746	0.335	0.152
1c, **1g**	4.818	2.130	0.9875	0.746	0.335	

[a] The perturbation of the 2,7-proton coupling constant caused by deuteriation in the 1-, 3-, 6-, and 8-positions is real and is the subject of a separate article.[31]

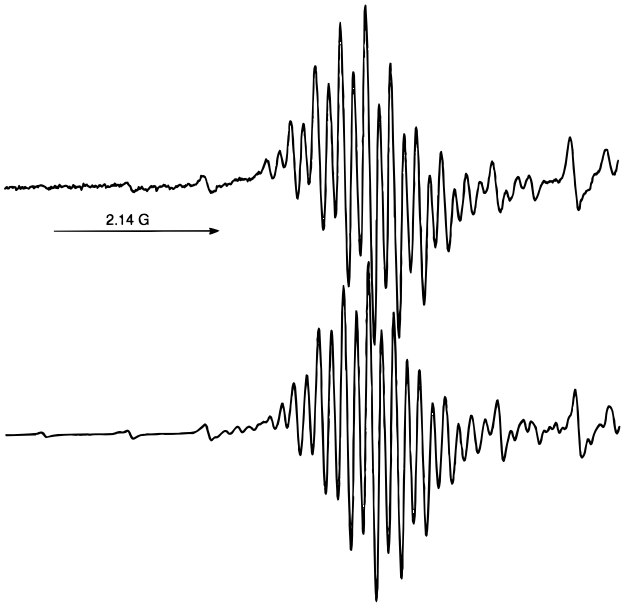

Figure 2. Upper: an 8 G section, starting just before the second $PY^{\bullet-}$ peak, of the EPR spectrum resulting from the K reduction of a mixture of our 2,4,5,7,9,10-d_6-pyrene sample mixed with pyrene ([2,4,5,7,9,10-d_6-PY]/[PY] = 52.1) at 173 K in THF. Lower: computer simulation assuming [2,4,5,7,9,10-d_6-$PY^{\bullet-}$]/[$PY^{\bullet-}$] = 27.3 and isotopic impurities at levels indicated in Table 1. PPW = 0.08 G.

$PY^{\bullet-}$]/[$PY^{\bullet-}$] = 27.3. The isotopic impurity anion radicals were included in the simulation in relative abundancies as described in Table 1. Electron transfer between various deuterio isomers may have altered these ratios somewhat. However, the presence of both more and less deuteriated isotopic "impurities" tends to average out any observable effect of this equilibration. In any event, the ΔEA between pyrene and a given deuteriated isomer is significantly larger than those between the given isomer and its major cosynthesized impurities. The K_{eq} for reaction 3 implied by this particular experiment is 27.3/(0.284/0.005 45) = $K_{eq(\mathbf{1f})}$ = 0.52.

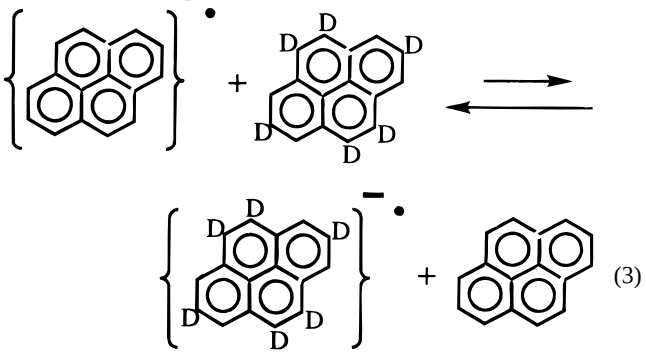

(3)

Repetition of the experiment yielded an average K_{eq} of 0.57 ± 0.06 at 173 K.

*1,2,3,6,7,8-d₆-Pyrene (**1e**).* The synthetic procedure used (see Experimental Section) resulted in a significant isotopic contamination at the 4-, 5-, 9-, and 10-positions of compound **1e**. Despite this, an excellent computer simulation of the EPR spectrum of the anion radical of this material was obtained (Figure 3) assuming the product to be 58.9% isotopically pure 1,2,3,6,7,8-d_6-PY and including the isotopic impurities at the levels indicated in Table 1.

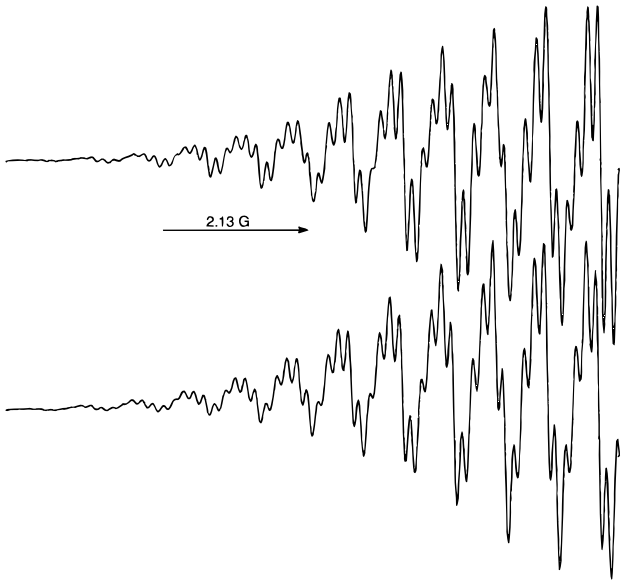

Figure 3. Upper: low-field half (9 G scan) of our reduced 1,2,3,6,7,8-d_6-PY product. Lower: computer simulation of this spectrum that is generated assuming the isotopic impurity levels given in Table 1 and the coupling constants shown in Table 2. PPW = 0.138 G.

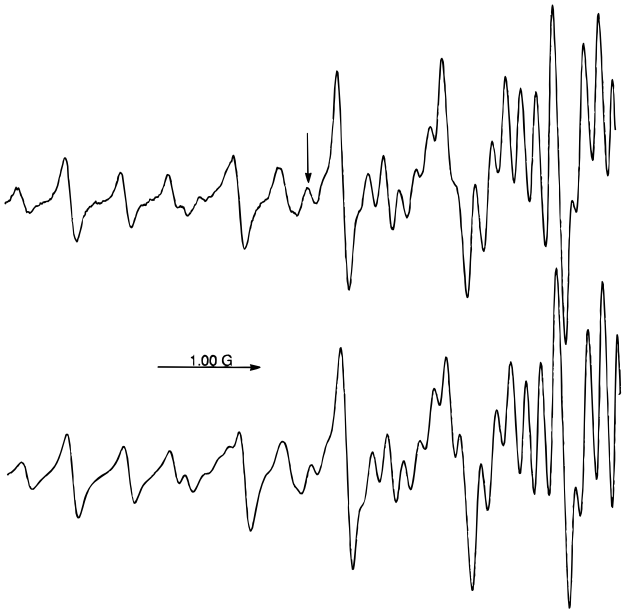

Figure 4. Upper: a 6 G scan of the EPR spectrum at 173 K of a mixture of 50.5 mg of our (impure) 1,2,3,6,7,8-d_6-PY sample containing 0.143 mmol of **1e** and 0.007 92 mmol of PY that has been partially reduced with potassium metal. This scan begins 3 G downfield from the first line corresponding to the anion radical of **1e**, indicated by the vertical arrow. Lower: computer simulation generated implying an equilibrium constant for reaction 1 (A = pyrene and *A = **1e**) of 0.43. The relative concentrations of **1e** and isotopic impurities are included as shown in Table 1. PPW = 0.105 G.

When a mixture of 50.5 mg of our (isotopically impure) 1,2,3,6,7,8-d_6-PY sample (50.5 × 0.589/208 = 0.143 mmol of **1e**) and 1.6 mg (0.007 92 mmol) of PY is partially reduced, the resulting EPR spectrum is best simulated (Figure 4) utilizing a ratio [1,2,3,6,7,8-d_6-$PY^{\bullet-}$]/[$PY^{\bullet-}$] of 7.83. This implies an equilibrium constant for reaction 1, where A and *A represent

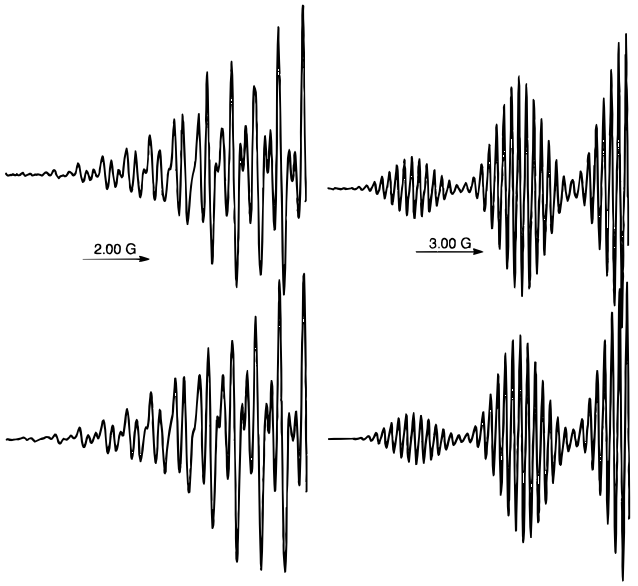

Figure 5. Upper: low-field halves of the EPR spectra of solutions resulting from the reduction of our 1,3,6,8-d_4-PY (left, 9 G scan) and 4,5,9,10-d_4-PY (right, 13.5 G scan). Lower: computer simulations of these spectra that are generated by including the isotopic impurities given in Table 1 and utilizing the coupling constants shown in Table 2. PPW = 0.125 G on the left and PPW = 0.110 G on the right.

pyrene and 1,2,3,6,7,8-d_6-PY respectively, of 7.83/(0.143/0.007 92) = 0.43. Repetition yielded an average value for $K_{\text{eq(1e)}}$ of 0.42 ± 0.05 at 173 K.

1c and 1d. Each of these materials was treated as described for **1e** and **1f** in a manner that is consistent with the results in Tables 1 and 2 and Figure 5. The equilibrium constants at 173 K for reaction 1 are 0.43 ± 0.04 and 0.63 ± 0.04 when *A = 1,3,6,8-d_4-PY and 4,5,9,10-d_4-PY, respectively.

1g and 1b. Each of these materials was treated as described for **1e** and **1f** in a manner that is consistent with the values in Tables 1 and 2. The EPR analysis of mixtures of our 1,3,4,5,6,8,9,10-d_8-pyrene sample and pyrene reveals that the equilibrium constant for reaction 1 is 0.37 ± 0.04 when *A = 1,3,4,5,6,8,9,10-d_8-PY (Figure 6). This system represents our most highly substituted synthesized deuterio pyrene. The least deuterium-substituted synthesized pyrene is represented by structure **1b**, and K_{eq} at 173 K for reaction 1 when *A = 2,7-d_2-PY is 0.80 ± 0.04, (Figure 6).

1h. The perdeuteriated PY (used as supplied from Aldrich Chemical Co.) was assumed to be 100% isotopically pure. The equilibrium constant at 173 K for reaction 1 when *A = **1h** was found to be 0.25 ± 0.04. This value is lower than that previously reported (0.37 ± 0.06)[7] and is based upon more data and a more sophisticated analysis.

Voltammetric Experiments. Any difference in the reduction potentials of A and *A (reaction 1) means that the equilibrium constant deviates from unity. In *N*,*N*-dimethylformamide (DMF) containing 0.1 M tetra-*n*-butylammonium hexafluorophosphate, the deuteriated pyrenes were invariably found to be more difficult to reduce than pyrene itself. The largest difference observed, 12.4 mV, was that between perdeuteriated pyrene (**1h**) and pyrene (**1a**), which translates ($\Delta G° = -nF\Delta E°$) into a difference in solution electron affinities of 1197 J/mol. Identical experiments carried out on compounds **1a**−**1h** yield potential differences, tabulated in Table 3, ranging from 1.5 to 12.4 mV with standard deviations between 0.2 and 0.4 mV.

MO Calculations. The isotope effects on the one-electron affinity were calculated as perturbations (due to isotopic substitution) upon the zero-point energy differences between the various neutral and radical anionic species. These isotope effects have been calculated using the PM3 parametrization[12] with three different formalisms: restricted open-shell Hartree−Fock (ROHF), unrestricted Hartree−Fock (UHF), and annihilated unrestricted Hartree−Fock (AUHF) theories.[14] Previous calculations on benzene/benzene radical anions using the UHF formalism for the radical anions accounted for 50−60% of the experimentally observed ΔEA values and reproduced geometrical distortions (symmetry lowering from D_{6h} to C_{2h} on reduction) correctly as well. However, for the one-electron reduction of cyclooctatetraene the UHF calculations did not predict the experimental geometry of the radical anion correctly, while the ROHF formalism did. Therefore, results based upon all three available formalisms are reported (Table 4).

The charge distributions in pyrene and the radical anion of pyrene have been calculated as well and are given for the carbon positions where hydrogen atoms are attached in Table 5. The calculated values of the charges depend on where the electron cloud is "cut" between the atoms that share these electrons. Therefore, the reported data must be considered to be charge-indicators rather than absolute values. Many more or less elaborate schemes for obtaining the "correct" atomic charge have been published, but disputes are still going on concerning which procedure is best in which case.[15] We have therefore used the standard data as obtained from the VAMP and MOPAC programs.[16] In parentheses are added the so-called light-in-heavy charges in which the charge on the hydrogen atom is

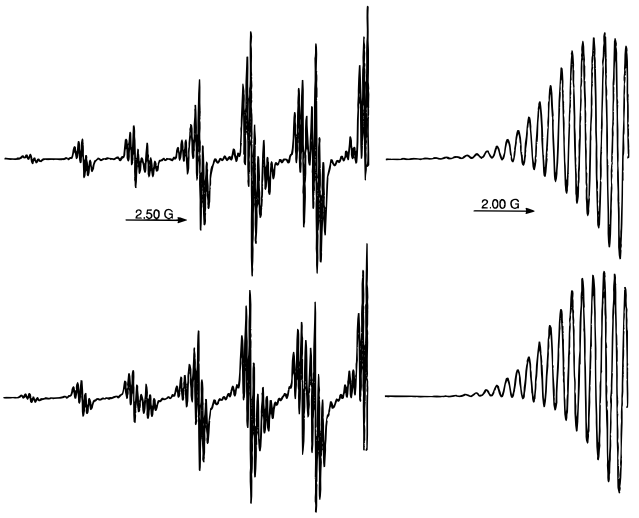

Figure 6. Upper: low-field halves of the EPR spectra of solutions resulting from the reduction of our 2,7-d_2-PY (left, 15 G scan) and 1,3,4,5,6,8,9,10-d_8-PY (right, 8 G scan). Lower: computer simulations of these spectra that are generated by including the (essential) isotopic impurities given in Table 1 and utilizing the coupling constants shown in Table 2. PPW = 0.095 G on the left, and PPW = 0.140 G on the right.

TABLE 3: Potential Differences and Electrochemical (in DMF), EPR (in THF), and Theoretical Relative Solution Electron Affinities ($\Delta G°$ = ΔEA for Reaction 1) of the Various Deuteriated Pyrenes Relative to That of Pyrene

ΔE_p, mV	ΔEA_{EL}, J/mol	ΔEA_{EPR}, J/mol	ΔEA_{ROHF}, J/mol	*A
0	0	0	0	PY (**1a**)
1.5 ± 0.2	145	320	17	2,7-***d***$_2$-PY (**1b**)
6.8 ± 0.2	656	1240	242	1,3,6,8-d_4-PY (**1c**)
3.2 ± 0.2	309	668	84	4,5,9,10-d_4-PY (**1d**)
7.5 ± 0.4	724	1210	268	1,2,3,6,7,8-d_6-PY (**1e**)
5.4 ± 0.3	521	813	105	2,4,5,7,9,10-d_6-PY (**1f**)
10.0 ± 0.2	965	1430	334	1,3,4,5,6,8,9,10-d_8-PY (**1g**)
12.4 ± 0.3	1197	1990	355	d_{10}-PY (**1h**)

TABLE 4: Difference in Electron Affinity with Respect to All-H Pyrene (ΔEA in J/mol), as Obtained from PM3 Calculations

compound	substitution pattern	ΔEA_{ROHF}	ΔEA_{UHF}	ΔEA_{AUHF}
1a	d_0	0	0	0
1b	2,7-d_2	17	79	29
1c	1,3,6,8-d_4	242	401	251
1d	4,5,9,10-d_4	84	75	84
1e	1,2,3,6,7,8-d_6	268	485	276
1f	2,4,5,7,9,10-d_6	105	159	109
1g	1,3,4,5,6,8,9,10-d_8	334	485	330
1h	d_{10}	355	560	355

TABLE 5: Calculated and Light-in-Heavy (in Parentheses) Charges at the Carbons in Pyrene and Pyrene Radical Anion by the Various Methods

position	PY	$PY^{\bullet-}$ (ROHF)	$PY^{\bullet-}$ (UHF)	$PY^{\bullet-}$ (AUHF)
C1	−0.09 (+0.02)	−0.25 (−0.16)	−0.22 (−0.13)	−0.25 (−0.16)
C2	−0.10 (+0.00)	−0.05 (+0.01)	−0.07 (−0.01)	−0.05 (+0.01)
C4	−0.09 (+0.02)	−0.16 (−0.08)	−0.16 (−0.08)	−0.16 (−0.08)

TABLE 6: Calculated Charge Differences with the Corresponding Carbon Atoms in Neutral Pyrene and the Light-in-Heavy Charge Differences (in Parentheses)

position	$PY^{\bullet-}$ (ROHF)	$PY^{\bullet-}$ (UHF)	$PY^{\bullet-}$(AUHF)
C1	−0.16 (−0.18)	−0.13 (−0.15)	−0.16 (−0.18)
C2	+0.05 (+0.01)	+0.03 (−0.01)	+0.05 (+0.01)
C4	−0.07 (−0.10)	−0.07 (−0.10)	−0.07 (−0.10)

added to that of the carbon atom to which it is attached. In any case this has the advantage that one less arbitrary boundary has to be assumed (that between the electron clouds of a carbon atom and the attached hydrogen).

The data in Table 5 give rise to those in Table 6, which presents differences in the charge densities between the pyrene anion radical and the neutral pyrene for each of the three formalisms. The charge differences are presumably slightly more reliable as charge-indicators because of a partial cancellation of errors.

Discussion

The data in Table 3 show a gradual increase in ΔEA with increasing deuteriation of pyrene and that the CV and EPR data are within experimental error of being collinear (Figure 7). The smallest value for ΔEA (K_{eq} closest to 1.00) is observed for 2,7-d_2-pyrene. For vibrationally uncoupled L atoms (L = H, D), the measured values of K_{eq} are expected to follow the isotopic product rule.[17] The rule applies reasonably well for the 2,4,5,7,9,10-d_6 pyrene (**1f**) system. The product of $K_{eq(EPR,\mathbf{1b})} \times K_{eq(EPR,\mathbf{1d})} = 0.50$, which is slightly smaller than the experimentally observed 0.57 for $K_{eq(EPR,\mathbf{1f})}$. For the electrochemical experiments, $K_{eq(CV,\mathbf{1b})} \times K_{eq(CV,\mathbf{1d})} = 0.83$, which agrees well with 0.80 measured for $K_{eq(CV,\mathbf{1f})}$. The deviation from the product rule is somewhat larger for isotopic isomers in which both the 1- and 2-positions are deuteriated. Deviations from the isotopic product rule are to be expected because of an accumulation of factors such as imperfect EPR simulations of mixtures, incomplete knowledge regarding isotopic impurities, and vibrational coupling between L atoms at adjacent carbon atoms. We estimate that all of these to lead to about ±10% uncertainty in K_{eq} values. Propagated ranges in product K_{eq} values overlap those of averaged, measured K_{eq} values, and the isotopic product rule[17] holds reasonably well.

Assuming this rule holds, one can predict the experimental K_{eq} value for monodeuteriation on each of the three distinct positions in the molecule. For compounds **1b**−**1d** these values follow from taking the square root (**1b**) or fourth root (**1c** and **1d**) of the experimental K_{eq} values. For compounds with deuterium atoms at several distinct positions, to predict the expected contribution of the deuterium atoms at a position, one must compensate for the contribution of the deuterium atoms at other positions. For example, $K_{eq(EPR,\mathbf{1e})} = 0.42$. This leads to a value of $K_{eq(EPR,\mathbf{1e})}/K_{eq(EPR,\mathbf{1b})} = 0.42/0.80 = 0.52$ for the contribution to the K_{eq} value of the deuterium atoms at the 1-positions, which implies $K_{eq} = (0.52)^{1/4} = 0.85$ for a single deuterium at that position. If all experimental data are treated this way, this yields four K_{eq} values for monodeuteriation at each position, and averaging leads to K_{eq} values of 0.85, 0.94, and 0.91 for monodeuteriation at the 1-, 2-, and 4-positions, respectively. In the case of the electrochemical experiments these values are 0.94, 0.97, and 0.93, respectively. The experimental (EPR and less clearly, electrochemical) data suggest that the isotope effect is largest for deuteriation at the 1-positions. Monodeuteriation at the 2- and 4-positions leads to isotope effects that are similar in size, with the effect at the 4-positions perhaps just slightly larger. The computational data (Table 4) lead to the same conclusion.

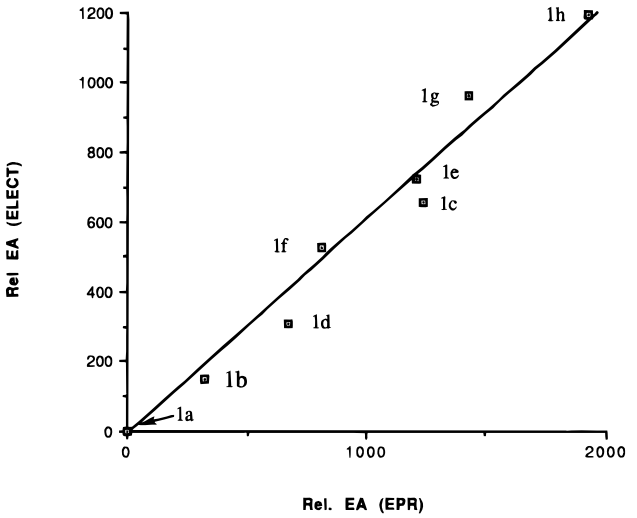

Figure 7. Plot of ΔEA determined electrochemically in DMF with tetrabutylammonium hexafluorophosphate at 294 K vs ΔEA determined via EPR in THF with K^+ serving as the counterion at 173 K. The linear correlation constant is 0.987, and the line fits the equation $\Delta EA_{ELECT} = 0.61\Delta EA_{EPR} - 8.99$.

For comparison of the experimental and theoretical (multideuteriated) data, the $\Delta G°$'s ($\Delta G° = \Delta EA$) for the electron transfer reaction (at 173 K) from the ROHF data are graphically presented in Figure 8. The AUHF data are almost identical to the ROHF data and will not be discussed separately.

The plot shown in Figure 8 and the data in Table 3 lead to two conclusions. First, a correlation between the experimental and calculated values is observed. This means that the effects of isotopic substitution on the one-electron-accepting ability of pyrene are reflected well by the PM3 calculations, irrespective of the method (ROHF or UHF) used. The underlying assumption that ΔEA is an intrinsic property of the pyrene/pyrene radical anion couple, and dominated by ZPE differences, therefore passes the experimental test. Second, Figure 8 shows that the calculations significantly underestimate the values of ΔEA (the slopes are not unity). However, the observed linear correlation means that theoretically obtained data can be usefully compared to the experimental data since the relevant properties are underestimated theoretically by a constant proportion.

The calculations, of course, do not attempt to account for the effects of solvation or ion association. Thus, in order for the slopes of the lines shown in Figure 8 to be unity, the

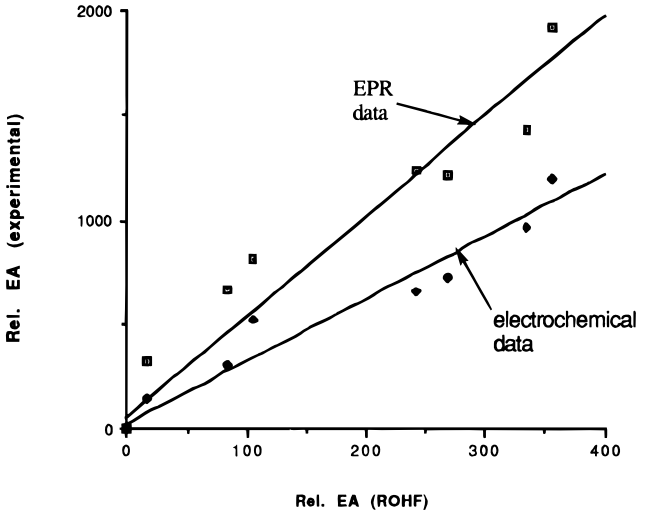

Figure 8. Plots of the experimental (EPR, upper, and electrochemical, lower) free energy changes for the electron transfer (ΔEA) from the pyrene anion radical to the various deuteriated pyrenes vs the ROHF calculated values. The lines fit the equations $\Delta EA_{EPR} = 4.8\Delta EA_{ROHF} + 49$ and $\Delta EA_{ELECT} = 3.0\Delta EA_{ROHF} + 18$. The correlation constants are 0.96 (EPR) and 0.97 (ELECT).

enthalpies (and free energies) of solvation of the products and the reactants of reaction 1 must be identical. The enthalpy of solvation of the pyrene anion radical plus K^+ in THF ($\Delta H°_{sol}$ for reaction 4) is −765 kJ/mol.[18]

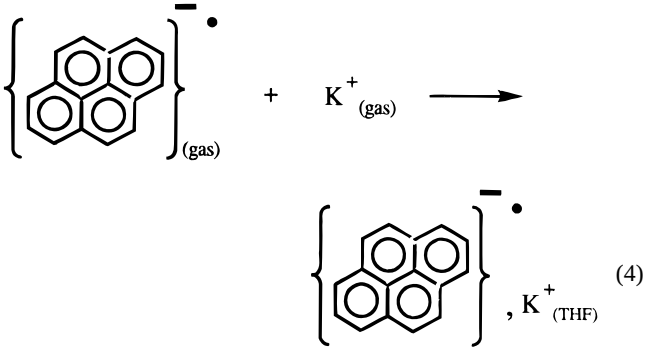

(4)

If deuteriation perturbed the enthalpy for reaction 4 by as little as several hundred J/mol (or *a few hundredths of 1%*), it would be sufficient to result in the slopes of the lines shown in Figure 8 deviating from unity to the degree that they do. Indeed, preliminary MO calculations using the program MOPAC 7 indicate that this is the case and yield a difference in the solvation of the pyrene and perdeuteriated pyrene anion radicals in DMF of about 1 kJ/mol. Furthermore, the fact that the slope of the line shown in Figure 7 is only 0.6 probably reflects the fact that these ion association and solvation effects are greater in THF with K^+ serving as the counterion than in DMF with $(C_4H_9)_4N^+$.

The hypothesis that a relation exists between the observed equilibrium isotope effect and the charge developed on the hydrogen/deuterium substituted carbon atom was tested by comparing the experimental results to the calculated atomic charges in Table 5. All three formalisms used indicate the order of negative charge on the L-atom-substituted carbon atoms in the radical anion to be C1 > C4 > C2, irrespective of taking the calculated charges or the light-summed-in-heavy charges as charge-indicators. The charge differences (Table 6) also show the same order: the development of negative charge is largest on C1, and the next largest is on C4. For C2, development of a slightly less negative charge is calculated with all methods. By use of the hydrogen-summed-into-carbon charges, the charge on C2 stays about constant upon reduction of pyrene. Although the isotope effect of monodeuteriation is largest at the 1-positions, which carry the highest negative charge, such a correlation is not evident for the isotope effects at the other two positions. The negative charge on C4 is calculated to be substantially larger than that on C2, but the isotope effect *per deuterium* at those two positions is about equal according to results from both theory and experiment. According to the experimental and ROHF data $\Delta EA(2\text{-}d_1) \leq \Delta EA(4\text{-}d_1)$, while the UHF results predict $\Delta EA(2\text{-}d_1) \geq \Delta EA(4\text{-}d_1)$. It is therefore concluded that no evidence for a general relation between ΔEA and the charge on the carbon atom at which the deuterium atom resides is observed.

Conclusions

The experimental (electrochemical and EPR) and theoretical (PM3) data on the isotope effect on the electron affinity for a series of partially deuteriated pyrene isotopic isomers show a gradual increase in ΔEA with increasing deuterium substitution. The correlation between the electrochemical data and the EPR data is excellent. The experimental and theoretical data correlate well, which is strong evidence for the applicability of the theoretical method used. No evidence is found for a general relation between the value of ΔEA and the charge on the carbon atom that carries a hydrogen or deuterium atom. The nonunity slopes of the lines shown in Figures 7 and 8, as well as MOPAC 7 calculations, suggest that ion association and ion solvation are slightly different for the deuteriated and nondeuteriated anion radicals of pyrene.

Experimental Section

Synthesis. Six newly described isotopic isomers of pyrene were synthesized, namely 2,7-di- (**1b**), 1,3,6,8-tetra- (**1c**), 4,5,9,10-tetra- (**1d**), 1,2,3,6,7,8-hexa- (**1e**), 2,4,5,7,9,10-hexa- (**1f**), and 1,3,4,5,6,8,9,10-octadeuteriopyrene (**1g**). The strategy used was that of repeated acidic exchange of the arene hydrogens or basic exchange of the benzylic hydrogens in 4,5,9,10-tetrahydropyrene (**2**) and 1,2,3,6,7,8-hexahydropyrene (**3**) in deuteriated solvents. These procedures followed by dehydrogenation yielded **1d**, **1e**, and **1g**. Selective replacement of deuteriums by hydrogens via a two-step procedure of bromination and subsequent debromination yielded **1b**, **1c**, and **1f**.

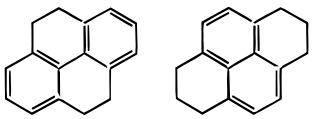

2 **3**

Deuterium exchange reactions in acidic media on polycyclic aromatic hydrocarbons are often performed using deuteriotrifluoroacetic acid[19] or concentrated deuteriosulfuric acid.[20] For preparative purposes it appeared advantageous to use another deuterium-exchange medium: deuteriated poly(phosphoric acid) (PPA-*d*).[21] The advantages of PPA-*d* as a deuterium-donating agent are the following: (1) it can be easily prepared, at a large scale, from D_2O and P_2O_5, which are relatively cheap materials; (2) it can be heated to relatively high temperatures (>200 °C), which is useful in slow exchange reactions; (3) it is not an oxidizing agent and does not enter into aromatic substitutions.

Deuterium oxide (99.9% D) and DMSO-d_6 (99.5% D) were purchased from Aldrich. Pyrene (99%) was obtained from Janssen Chimica. 1,2,3,6,7,8-Hexahydropyrene (**3**) was prepared by reduction of pyrene with Na in refluxing isoamyl

alcohol,[22] and 4,5,9,10-tetrahydropyrene (**2**) was prepared analogously from 4,5-dihydropyrene in refluxing toluene.[23] 4,5-Dihydropyrene was purified by column chromatography prior to reaction, in order to remove a small amount of pyrene. In this way the formation of **3** during the reduction was avoided. All solvents were distilled before use and dried if necessary. Silica gel (230−400 mesh) was obtained from Merck and used in all column chromatographic purifications. Petroleum ether with a boiling range 40−60 °C was used as an eluant.

The 300 MHz ^{1}H NMR and 46.9 MHz ^{2}H NMR spectra were recorded on a Bruker WM-300 spectrometer. In the ^{1}H NMR spectra TMS was used as an internal standard (0 ppm) and $CDCl_3$ (99.8% D) as a solvent. Concentrations were typically 2 mg/mL. In the ^{2}H NMR spectra $CDCl_3$ was used as a standard (7.26 ppm) and $CHCl_3$ or CCl_4 as a solvent. Concentrations were typically 40 mg/mL. Deuterium incorporations were calculated by intergration of the proton and deuterium signals. IR spectra were recorded on a Pye-Unicam SP3-200. Accurate molecular masses were determined by electron impact mass spectrometry using a V. G. Micromass ZAB-HFqQ mass spectrometer coupled to a V. G. 11/250 data system. The samples were introduced via the direct insertion probe into the ion source.

Deuteriated PPA was prepared by adding P_2O_5 (500 g) in small portions to D_2O (100 g) under mechanical stirring. An alcohol/dry ice bath was used to keep the temperature below 50 °C. When the addition was complete, the coolant was removed and the reaction mixture stirred for 2 h at 180 °C to dissolve all remaining P_2O_5. The prepared amount of PPA-*d* was transferred into six 50 mL round-bottom flasks while still warm. A stirrer bar was added to each flask, and the flasks were closed, allowed to cool, sealed, and stored.

*Perdeuteriopyrene (**1h**).* Perdeuteriopyrene was synthesized by portionwise addition of pyrene (3.06 g; 15.0 mmol) to a round-bottom flask containing approximately 90 g of PPA-*d* under vigorous stirring at 190−200 °C. After 4 h of stirring the reaction mixture was allowed to cool to 100 °C, and the dark mixture was poured over ice (500 g) and extracted twice with CH_2Cl_2. The combined organic layers were washed with a solution of Na_2CO_3 and dried ($MgSO_4$). The solvent was evaporated. After the first and second exchange cycle purification was confined to a rapid cleanup of the brown product over a small amount of silica gel (elution with petroleum ether). The final, third exchange cycle was followed by regular column chromatography and yielded 2.03 g (60%) of **1h**. Deuterium incorporation at each position as determined by NMR and mass spectrometry (MS) was >98%. IR (KBr): 1555, 1422, 1331, 1275, 1037, 946, 810, 743 cm^{-1}. MS (*m*/*z*): $M^+ = 212.1448$ ($C_{16}D_{10}$ requires 212.1410).

*2,4,5,7,9,10-Hexadeuteriopyrene (**1f**).* Perdeuteriopyrene (0.98 g; 4.6 mmol) was brominated with Br_2 (3.3 g; 20.6 mmol) in nitrobenzene (40 mL).[24] 1,3,6,8-Tetrabromo-2,4,5,7,9,10-hexadeuteriopyrene (2.24 g; 100%) was collected as a light-green powder and was not purified further. To this solid, tetrahydrofuran (100 mL) was added, and the resulting suspension was cooled with an ice-bath. $LiAlH_4$ (700 mg; 18.4 mmol) was added under stirring. $TiCl_4$ (900 mg; 4.7 mmol) was cautiously added, whereupon the reaction mixture turned dark-brown immediately. After 30 min the coolant was removed, and stirring was continued for another 90 min at room temperature. The reaction mixture was poured on ice and extracted twice with diethyl ether. The combined organic layers were dried ($MgSO_4$), and the solvent was evaporated. The resulting yellow residue was purified with column chromatography. 2,4,5,7,9,10-Hexadeuteropyrene (**1f**) was isolated as white crystals (550 mg; 57%). ^{1}H and ^{2}H NMR show a deuterium incorporation of 98% at positions 2, 4, 5, 7, 9, and 10 and of 5% at positions 1, 3, 6, and 8. IR (KBr): 1580, 1433, 1018, 889, 675 cm^{-1}. MS (*m*/*z*): $M^+ = 208.1196$ ($C_{16}H_4D_6$ requires 208.1159).

*1,2,3,6,7,8-Hexadeuterio-4,5,9,10-tetrahydropyrene (**2e**).* 4,5,9,10-Tetrahydropyrene (**2a**) (10.0 g; 48.4 mmol) was deuteriated 3 times with PPA-*d* (90 g) in the manner described for pyrene. The reaction was carried out at 160 °C for 3 h. After purification (silica; petroleum ether) **2e** was obtained as white plates (6.5 g; 63%). According to NMR, the deuterium incorporation at the aromatic positions is 98%. On the benzylic positions approximately 10% deuterium is incorporated. IR (KBr): 2915, 2880, 2820, 2245, 1427, 1377, 1210, 1194, 833, 810 cm^{-1}. MS (*m*/*z*): $M^+ = 212.1449$ ($C_{16}H_8D_6$ requires 212.1472).

*1,2,3,6,7,8-Hexadeuteriopyrene (**1e**).* To a solution of **2e** (3.10 g; 14.6 mmol) in dry toluene (100 mL) DDQ (7.4 g; 32.8 mmol) was added. The reaction mixture was refluxed under an argon atmosphere for 2 h. After the mixture had cooled to room temperature it was filtered over Hyflo. The organic layer was washed twice with a solution of Na_2CO_3 and dried over $MgSO_4$; the solvent was evaporated in vacuo. Column chromatography yielded **1e** as white crystals (2.65 g; 87%). ^{1}H and ^{2}H NMR give a deuterium incorporation at positions 1, 2, 3, 6, 7, and 8 of 97% and at positions 4, 5, 9, and 10 of about 10%. IR (KBr): 1560, 1290, 1154, 832, 780, 694 cm^{-1}. MS (*m*/*z*): $M^+ = 208.1136$ ($C_{16}H_4D_6$ requires 208.1159).

*2,7-Dideuteriopyrene (**1b**).* Compound **1e** (1.80 g; 8.6 mmol) was brominated and debrominated in the same way as outlined for perdeuteriopyrene. The yield of **1b** after purification was 960 mg (54%). Deuterium incorporation according to NMR is 97% at positions 2 and 7, 2% at positions 1, 3, 6, and 8, and about 10% at positions 4, 5, 9, and 10. IR (KBr): 1584, 1307, 1323, 1148, 1010, 895, 886, 810, 708, 678, 660 cm^{-1}. MS (*m*/*z*): $M^+ = 204.0931$ ($C_{16}H_8D_2$ requires 204.0908).

*1,3,6,8-Tetradeuterio-4,5,9,10-tetrahydropyrene (**2c**).* Compound **2e** (2.06 g; 9.7 mmol) was treated with Br_2 (3.5 g; 22 mmol) and $FeCl_3 \cdot 6H_2O$ (270 mg; 1.0 mmol) in water (75 mL).[25] After recrystallization (cyclohexane) 2,7-dibromo-1,3,6,8-tetradeuterio-4,5,9,10-tetrahydropyrene was obtained as white crystals in 1.45g (40%) yield. A 1.40 g (3.8 mmol) sample of this compound was reacted with $LiAlH_4$ (320 mg; 8.1 mmol) and $TiCl_4$ (380 mg; 2.0 mmol) in THF (75 mL) as described for the preparation of **1f**. The mixture was refluxed for 3 h to complete the reduction. Compound **2c** was obtained in 660 mg (83%) yield. It was dissolved in DMSO (6 mL) and added to a NaH suspension (500 mg, 50% in paraffin oil, twice washed with 10 mL of cyclohexane). The reaction mixture was heated to 90−95 °C at which temperature evolution of H_2 took place. After 2 h the dark-brown suspension was allowed to cool to room temperature. Water was added, and the mixture was extracted twice with CH_2Cl_2. The combined organic layers were washed with water and dried over $MgSO_4$; the solvent was evaporated in vacuo. Purification by column chromatography yielded **2c** as white crystals (590 mg; 90%). Deuterium incorporation (NMR) was 95% at positions 1, 3, 6, and 8 and ≤1% at positions 2, 4, 5, 7, 9, and 10. IR (KBr): 2915, 2880, 2825, 2245, 1426, 1411, 1294, 908 cm^{-1}. MS (*m*/*z*): $M^+ = 210.1379$ ($C_{16}D_{10}H_4$ requires 210.1347).

*1,3,6,8-Tetradeuteriopyrene (**1d**).* Compound **2c** (580 mg; 2.75 mmol) was dehydrogenated with DDQ (1.36 g; 6.0 mmol) in refluxing toluene as described for the preparation of **1e**. The yield after purification was 425 mg (77%). Deuterium incorporation (NMR) was 95% at positions 1, 3, 6, and 8 and ≤1% at positions 2, 4, 5, 7, 9, and 10. IR (KBr): 1586, 1385, 1282,

1193, 1148, 959, 910, 827, 720 cm^{-1}. MS (*m*/*z*): M^+ = 206.1073 ($C_{16}H_6D_4$ requires 206.1034).

*4,5,9,10-Tetradeuterio-1,2,3,6,7,8-hexahydropyrene (**3d**).* 1,2,3,6,7,8,-Hexahydropyrene (**3**) (5.9 g; 28.4 mmol) was deuteriated twice with PPA-*d* (90g) as described for pyrene (160 °C, 3h). Compound **3d** was collected after column chromatography as white plates (4.7 g; 78%). Deuterium incorporation (NMR) was 97% at positions 4, 5, 9, and 10, 12% at positions 1, 3, 6, and 8, and 9% at positions 2 and 7. IR (KBr): 2900, 2840, 2195, 1560, 1441, 1380, 1326, 1291, 1256, 1060, 896, 910 cm^{-1}. MS (*m*/*z*): M^+ = 212.1537 ($C_{16}H_{12}D_4$ requires 212.1503).

*1,1′,3,3′,4,5,6,6′,8,8′,9,10-Dodecadeuterio-1,2,3,6,7,8-hexahydropyrene (**3g**).* Compound **3d** (3.0 g; 14.2 mmol) was deuteriated twice with DMSO-d_6 (20 g) and NaH (3.0 g, 50% dispersion in paraffin oil) for 20 h.[26] Column chromatography yielded 2.10 g (67%) of pure **3g**. Deuterium incorporation (NMR) was 97% at positions 1, 3, 4, 5, 6, 8, 9, and 10 and 12% at positions 2 and 7. IR (KBr): 2895, 2840, 2240, 2190, 2090, 1553, 1450, 1382, 1317, 1171, 1053, 902, 843, 644 cm^{-1}. MS (*m*/*z*): M^+ = 220.2036 ($C_{16}H_4D_{12}$ requires 220.2005).

*1,3,4,5,6,8,9,10-Octadeuteriopyrene (**1g**).* Compound **3g** (1.95 g; 8.9 mmol) was dehydrogenated with DDQ (6.3 g; 27.9 mmol) in refluxing toluene as described for **1e**, yielding after column chromatography **1g** (1.56 g; 83%) as white crystals. Deuterium incorporation (NMR) was 97% at positions 1, 3, 6, and 8, 95% at positions 4, 5, 9, and 10, and 12% at positions 2 and 7. IR (KBr): 1560, 1278, 922, 840, 789 cm^{-1}. MS (*m*/*z*): M^+ = 210.1261 ($C_{16}H_2D_8$ requires 210.1285).

*4,5,9,10-Tetradeuteriopyrene (**1d**).* Compound **1g** (950 mg; 4.5 mmol) was subjected to the bromination/debromination sequence as outlined for the preparation of **1f**. Compound **1d** was obtained after purification in 435 mg (46%) yield. Deuterium incorporation (NMR) was 95% at positions 4, 5, 9, and 10, 3% at positions 1, 3, 6, and 8, and 9% at positions 2 and 7. IR (KBr): 1585, 1428, 1157, 890, 804, 725, 675 cm^{-1}. MS (*m*/*z*): M^+ = 206.1028 ($C_{16}H_6D_4$ requires 206.1034).

EPR Measurements. EPR measurements were carried out as previously described on an IBM (Bruker) ER-200D spectrometer equipped with an IBM variable temperature unit[11f] and simulated.[27] It is important to note that the K_{eq}'s determined via the EPR measurements lie within the experimental error reported only if less than 10% of the pyrenes are reduced in the partial reductions, that is, when $[*A^{\bullet -}]$ and $[A^{\bullet -}] \ll [*A]_0$ and $[A]_0$, where $[*A]_0$ and $[A]_0$ represent the total concentrations of deuteriated pyrene and pyrene used in the reaction. The ratio $[A*]_0/[A]_0$ was obtained by careful weighing of the two materials. Each reported K_{eq} is an average based upon three to six such isotopic ratios.

Electrochemistry. *N*,*N*-Dimethylformamide (LAB-SCAN, HPLC grade) was distilled under reduced pressure prior to use. Tetrabutylammonium hexafluorophosphate was prepared by a procedure analogous to that described earlier for the tetrafluoroborate salt.[28]

The voltammetry cell was a cylindrical tube (50 mL) with a NS29 joint to accommodate a plastic holder for the three electrodes and the nitrogen inlet. The working electrode was prepared by sealing a 0.6 mm platinum wire in glass and polishing to obtain a planar surface. The electrode was electrochemically covered with mercury by serving as a cathode in a solution of mercuric nitrate in dilute aqueous nitric acid. The reference electrode, consisting of an Ag-wire in DMF containing Bu_4NPF_6 (0.1 M) was prepared as described by Moe[29] and stored until the potential was constant. The counterelectrode was a platinum wire sealed in soft glass. The potentiostat was a PAR Model 173/276 driven by an HP 3314A function generator. The function generator was activated periodically (in this study every 30 s) by a specially designed trigger operated in a mode that allowed every second measurement in a series to be delayed by 10 ms corresponding to a half-period of the 50 Hz sine wave of the power line.[30] In this way most of the noise from the power line in one measurement will be out of phase with the noise in the previous measurement and thus cancels when the average of these two measurements is taken. In addition, the high-frequency noise was reduced by filtering the output from the potentiostat by means of a PAR Model 189 selective amplifier. The current−voltage curves were recorded in the current−time mode on a 12-bit Nicolet oscilloscope, Model 2090-3C/206-2, with a horizontal resolution of 0.5 mV/point. The temperature was continuously monitored by a Philips PM2519 automatic multimeter equipped with a temperature probe. The function generator, the oscilloscope, and the multimeter were interfaced to an HP 9826A desk computer equipped with an HP 98635A floating point accelerator and an HP 9154A hard disk. The software used for instrument control and data-handling procedures (see below) was written in HP Basic 3.0.

The pyrene (0.02 mmol) was added to the voltammetry cell and dissolved in 10 mL of DMF containing Bu_4NPF_6 (0.1 M) by purging with nitrogen for at least 10 min. This also served the purpose of removing dissolved oxygen. The same solvent-supporting electrolyte stock solution was used for all eight pyrenes.

The undeuteriated pyrene (**1a**) served as an external standard during the voltammetric measurements, which were performed in an AA−BB−AA−BB−AA−BB−AA−CC−AA−CC−AA−CC−...−AA−HH−AA−HH−AA−HH−AA sequence, where each single letter refers to a series of measurements carried out as described below: A on the pyrene solution and B−H on the solutions of the seven deuteriated pyrenes (**1b**−**1h**). Thus, two series of measurements were carried out on each solution after which the electrode assembly was transferred to the next solution in the order described.

A series of measurements consisted of 10 current−time curves, each of which included an 800 mV negatively swept linear potential scan (10 V/s) initiated approximately 600 mV before the peak potential for the reduction of pyrene. The rate of the scan back to the start potential was 10 times that of the forward scan, i.e., 100 V/s, in order to diminish the time needed to record a single curve. The current−time curves were recorded at the oscilloscope and then transferred to the computer. Averages were taken for every two current−time curves (see above), resulting in five averaged curves: 1 and 2; 3 and 4; 5 and 6; 7 and 8; 9 and 10. The rest potential in the time interval between two measurements (ca. 30 s) was equal to the start potential.

Each of the averaged curves was processed as follows. First, an equation for the base line was estimated by linear regression of the data points recorded well in front of the rising part of the reduction wave. The base line was extrapolated to the potential region of the reduction peak and subtracted from the current−time curve. An approximate position of the peak located by the operator was used to define a ±20 mV data region around this peak, and the fitting of these data to a third-order polynomial followed by application of a maximizing procedure was then used to determine the peak current, I_p, and the peak potential, E_p. Linear regression of the data points in a ±15 mV region of the curve around the point corresponding most closely to $I = (1/2)I_p$ was finally used to determine the half-peak potential, $E_{p/2}$, as the value of E for which $I = (1/2)I_p$.

The entire measurement sequence gave rise to a set of six potential differences for each deuteriated pyrene, and the values given in Table 3 refer to the averages of these six values. The standard deviations were between 0.2 and 0.4 mV. The half-peak widths, $E_p - E_{p/2}$, were in most cases between 57.8 and 58.4 mV, typical for aromatic hydrocarbons at a scan rate of 10 V/s.

Calculations. The MO calculations were performed using the programs VAMP 4.30 (RHF, ROHF, and AUHF) and MOPAC 6 (UHF). Computation details have been previously published.[10]

Acknowledgment. The authors are grateful to R. Fokkens and H. Peeters, University of Amsterdam, J. van Houte and R. A. M. van der Hoeven, Leiden University, for the determination of the high-resolution mass spectrometric data and deuterium incorporations, and A. W. M. Lefeber, Leiden University, for the ^{2}H NMR measurements. C.D.S. thanks the National Science Foundation (Grant CHE-9412036) for support of this work. The electrochemical work was supported in part by The Danish Natural Science Research Council (Grant No. 11-0063). O.H. and M.F.N. gratefully acknowledge the receipt of funds from The Carlsberg Foundation and The Danish Natural Science Research Council for the purchase of the instrumentation.

References and Notes

(1) (a) Stevenson, G. R.; Espe, M. P.; Reiter, R. C. *J. Am. Chem. Soc.* **1986**, *108*, 532. (b) Morris, D. E.; Smith, W. H. *J. Electrochem. Soc*. **1991**, *138*, 1351. (c) Guthrie, R. D.; Shi, B. *J. Am. Chem. Soc*. **1990**, *112*, 3136. (d) Tanko, J. M.; Drumright, R. E. *J. Am. Chem. Soc*. **1992**, *114*, 1844. (e) Wen, X. L.; Liu, Z. L.; Liu, J. M.; Liu, Y. C. *J. Chem. Soc., Faraday Trans*. **1992**, *88*, 3323.

(2) Stevenson, G. R.; Sturgeon, B. E.; Vines, K. S.; Peters, S. J. *J. Phys. Chem.* **1988**, *92*, 6850.

(3) Stevenson, G. R.; Reiter, R. C.; Espe, M. P.; Bartmess, J. E. *J. Am. Chem. Soc.* **1987**, *109*, 3847.

(4) Stevenson, G. R.; Wehrmann, G. C., Jr.; Reiter, R. C. *J. Phys. Chem.* **1991**, *95*, 6936, and references therein.

(5) Goodnow, T. T.; Kaifer, A. E. *J. Phys. Chem.* **1990**, *94*, 7682.

(6) Stevenson, G. R.; Reidy, K. A.; Peters, S. J.; Reiter, R. C. *J. Am. Chem. Soc*. **1989**, *111*, 6578.

(7) Stevenson, G. R.; Sturgeon, B. E. *J. Org. Chem.* **1990**, *55*, 4090.

(8) Stevenson, G. R.; Wehrmann, G. C., Jr.; Reiter, R. C. *J. Phys. Chem.* **1991**, *95*, 901.

(9) Marx, D.; Kleinhesselink, D.; Wolfsberg, M. *J. Am. Chem. Soc.* **1989**, *111*, 1493.

(10) Zuilhof, H.; Lodder, G. *J. Phys. Chem.* **1992**, *96*, 6957.

(11) (a) Allendoerfer, R. D.; Papez, R. J. *J. Phys. Chem*. **1972**, *76*, 1012. (b) Lawler, R. G.; Tabit, C. T. *J. Am. Chem. Soc*. **1969**, *91*, 5671. (c) Hirota, N. *J. Phys. Chem*. **1967**, *71*, 127. (d) Stevenson, G. R.; Alegria, A. E. *J. Phys. Chem*. **1973**, *77*, 3100. (e) Kotake, Y.; Jansen, E. G. *J. Am. Chem. Soc*. **1989**, *111*, 5138. (f) Stevenson, C. D.; Halverson, T. D.; Reiter, R. C. *J. Am. Chem. Soc.* **1993**, *115*, 12405.

(12) (a) Stewart, J. J. P. *J. Comput. Chem.* **1989**, *10*, 209. (b) Stewart, J. J. P. *J. Comput. Chem.* **1989**, *10*, 221.

(13) The use of this technique for the heavy isotopically substituted systems has been criticized and is controversial; see ref 9.

(14) (a) Hurley, A. C. *Introduction to the Electron Theory of Small Molecules*; Academic Press: New York, 1976; pp 242−253. (b) Dewar, M. J. S. *The Molecular Orbital Theory of Organic Chemistry*; McGraw-Hill: New York, 1969; pp 250−277.

(15) Bachrach, S. M. *Rev. Comput. Chem*. **1994**, *5*, 171.

(16) Zuilhof, H.; Lodder, G. *J. Phys. Chem.* **1995**, *99*, 8033.

(17) Bigeleisen, J. *J. Chem. Phys*. **1955**, *23*, 2264.

(18) Stevenson, G. R.; Schock, L. E.; Reiter, R. C. *J. Phys. Chem.* **1983**, *87*, 4004.

(19) Mackor, E. L.; Hofstra, A.; Van der Waals, J. H. *Trans. Faraday Soc*. **1957**, *53*, 1309.

(20) Renaud, R. N.; Kovachic, D.; Leitch, L. C. *Can. J. Chem.* **1961**, *39*, 21.

(21) Gold, V.; Satchell, D. N. P. *J. Chem. Soc.* **1955**, 3622.

(22) Van den Braken-Van Leersum, A. M.; Tintel, C.; Van't Zelfde, M.; Cornelisse, J.; Lugtenburg, J. *Recl. Trav. Chim. Pays-Bas*, **1987**, *106*, 120.

(23) Rodenburg, L.; Floor, M.; Lefeber, A.; Cornelisse, J.; Lugtenburg, J. *Recl. Trav. Chim. Pays-Bas*, **1988**, *107*, 1.

(24) Volmann, H.; Becker, H.; Corell, M.; Streeck, H. *Justus Liebigs Ann. Chem.* **1937**, *531*, 1−159, synthesis on p 81.

(25) Lee, H.; Harvey, R. G. *J. Org. Chem.* **1986**, *51*, 2847.

(26) Chen, T.-S.; Wolinska-Macydiarz, J.; Leitch, L. C. *J. Labelled Compd.* **1970**, *6*, 285.

(27) (a) Morse, P. D. *EPRWare User Manual*; Scientific Software Services: Bloomington, Il., 1990. (b) Morse, P. D.; Reiter, R. C. *EWSim User Manual*; Scientific Software Services: Bloomington, Il., 1990.

(28) Nielsen, M. F.; Hammerich, O.; Parker, V. D. *Acta Chem. Scand., Ser. B* **1986**, *40*, 101.

(29) Moe, N. S. *Anal. Chem.* **1974**, *46*, 968.

(30) Nielsen, M. F.; Laursen, S. Aa.; Hammerich, O. *Acta Chem. Scand.* **1990**, *44*, 932.

(31) Zuilhof, H.; Lodder, G.; van Mill, R. P.; Mulder, P. P. J.; Kage, D.; Reiter, R. C.; Stevenson C. D. *J. Phys. Chem.* **1995**, *99*, 3461.

JP952098N